Astron. Astrophys. 174, 85–94 (1987)

ASTRONOMY AND ASTROPHYSICS

# A detailed analysis of the high energy gamma-ray emission from the Crab pulsar and nebula

**J. Clear[6], K. Bennett[6], R. Buccheri[3], I.A. Grenier[5], W. Hermsen[1], H.A. Mayer-Hasselwander[4], and B. Sacco[3]**

**The Caravane Collaboration for the COS-B satellite**

[1] Laboratory for Space Research Leiden, Leiden, The Netherlands
[2] Istituto di Fisica Cosmica del CNR, Milano, Italy
[3] Istituto di Fisica Cosmica e Informatica del CNR, Palermo, Italy
[4] Max-Planck-Institut für Physik und Astrophysik, Institut für Extraterrestrische Physik, D-8046 Garching-bei-München, Federal Republic of Germany
[5] Service d'Astrophysique, Centre d'Etudes Nucleaires de Saclay, Gif-sur-Yvette, France
[6] Space Science Department of the European Space Agency, ESTEC, 2200 AG Noordwijk, The Netherlands

Received July 21, accepted September 11, 1986

**Summary.** The results of a detailed analysis of the gamma ray emission from the Crab pulsar and nebula are reported. The data are the combination of 6 observations of the galactic anti-centre region made by COS-B in the energy range 50 MeV to 3000 MeV. The accumulation of the data over a period of 6.7 years from 1975 to 1982 has allowed a study of the temporal behaviour of the pulsed gamma ray flux from PSR 0531 + 21. A study of the ratio of the two gamma ray peaks in the pulsar's lightcurve shows evidence at a $3\sigma$ level for time variability over a scale of years. Fluctuations in the gamma ray flux from the pulsar have also been observed. For the first pulse the statistical significance of the fluctuations is not large enough ($2.0\sigma$) to claim variability. In the case of the second pulse a decrease in the flux during the period 1975–76 is observed. The significance of this variability is $3\sigma$. The spectrum of the pulsar emission can be represented by a single power law of index $2.00 \pm 0.10$ over the energy range of the instrument. No systematic variation of spectral index with pulsar phase has been noted. Unpulsed gamma ray emission from the Crab region has also been measured for energies up to 500 MeV. The spectrum of this emission may be represented by a single power law with spectral index of $2.7 \pm 0.3$ which supports the steeping of the spectrum observed in the hard X-ray range.

**Key words:** gamma rays – PSR 0531 + 21 – Crab nebula – COS-B

## 1. Introduction

The Crab Nebula is one of the most unusual and well studied celestial objects. Its emission has been observed from radio waves up to high energy gamma rays. The emission mechanism from the nebula is well understood, with synchrotron radiation from very high energy electrons moving in a magnetic field providing a good explanation for the observed spectrum. The discovery of the Crab pulsar has provided a source for the energy supply which is required to sustain the nebular emission, while the pulsar itself has also been observed throughout the electromagnetic spectrum with the emission being characterised by two pulses separated by approximately 0.4 in phase. The radiation from the pulsar is thought to result from the interaction of high energy particles with the intense magnetic fields that are known to exist at the surface of neutron stars, (see Knudt and Krotscheck, 1980 for a detailed review).

The Crab Nebula was the first identified celestial gamma ray source and its emission has been observed up to the highest gamma ray energies (Kniffen et al., 1974; Lichti et al., 1980; Cawley et al., 1985). The emission spectrum from the nebula can be represented by a single power law of index 2.08 from X-ray energies (Toor and Steward, 1974) up to energies of several MeV (Walraven et al., 1975), thus supporting the idea that synchroton radiation is the dominant emission process over this energy range. However, it has been proposed by some authors that the emission should depart from an extrapolation of the spectrum in the low energy gamma ray range with the spectral index changing from 2.1 to at least 2.3 (Laros et al., 1973) and recent results of Jung (1986) indicate a break in the nebular spectrum at 150 keV with the spectral index increasing to 2.54.

Since its discovery, the pulsar PSR 0531 + 21, has also been established as a source of pulsed gamma ray emission throughout the gamma ray spectrum: see for example Graser and Schönfelder (1982), 0.5–30 MeV; Kniffen et al. (1974), $\geq 30$ MeV; Bennett et al. (1977), 50–5000 MeV; Porter et al. (1974), $\geq 1$ TeV. At gamma ray energies the total emission spectrum from the pulsar may be represented by a single power law of index 2.1 (Bennett et al., 1977). However, at the highest energies (above 1 TeV) some softening of the spectrum is required (Dowthwaite et al., 1985).

A systematic variation in the pulsar spectral index with phase has been noted by Pravdo and Serlemitsos (1981) and it has been suggested that the pulsar emission may be represented by two independent components: (i) the emission from the two main peaks which dominates the pulsed emission over the entire energy spectrum and (ii) the emission from the interpulse which is just visible at optical energies but represents 15–30% of the pulsed emission from X-rays to high energy gamma rays. The emission spectrum from the first component is consistent with a synchrotron model, while the second component may be fitted by a bremmstrahlung or Compton model (Knight, 1982), or by curvature radiation (Hasinger, 1984).

*Send offprint requests to:* J. Clear

**Table 1.** Instrumental characteristics of each observation

| Observation period | Pointing direction $(l, b)$ | Aspect angle | Date | Relative efficiency | Exposure ($10^7$ cm$^2$ s) |
|---|---|---|---|---|---|
| 0 | 184°, −6° | 1° | 75/08/17<br>75/09/17 | 1.00 | 3.74 |
| 14 | 195°, +4° | 15° | 76/09/30<br>76/11/02 | 0.97 | 1.94 |
| 39 | 190°, 0° | 8° | 79/02/22<br>79/04/03 | 0.69 | 2.60 |
| 44 | 172°, −12° | 14° | 79/08/29<br>79/10/10 | 0.66 | 1.13 |
| 54 | 188°, −3° | 5° | 80/09/04<br>80/10/17 | 0.47 | 2.09 |
| 64 | 190°, 0° | 8° | 82/02/18<br>82/04/25 | 0.55 | 3.19 |

This paper reports the results of a detailed analysis of the total COS-B observations of the Crab region. With a total source exposure of $1.5\,10^8$ cm$^2$ s the data provide the largest gamma ray observations from the Crab region in this energy range. The long duration over which the data were accumulated (6.7 years) facilitates a study of the temporal behaviour of the gamma ray emission, while the good statistics available allow a measurement of the spectral index of the emission from both the pulsar and the nebula.

## 2. Observations

COS-B operated virtually continuously from its launch in 1975 until it was finally switched off in 1982. During these 6.7 yr 65 individual observations were made each lasting for a duration of approximately 30–40 d. Instrumental characteristics and operational details of the experiment have previously been given by Scarsi et al. (1977) and Mayer-Hasselwander (1985). By a selection of high quality gamma rays the observed data-set has been condensed to produce 'the final COS-B database' (Mayer-Hasselwander et al., 1985) which has been used for this analysis.

The Crab region was in the COS-B field of view during six of the observation periods. The details of each observation are given in Table 1. The observation period refers to the number of the particular observation within the COS-B data-set. The relative instrumental efficiency depicts the change in the detector sensitivity during the mission life-time. It is determined by a comparison of multiple observations of the galactic plane and is normalised to unity at the beginning of the experiment. The systematic uncertainty in the determination of this value is of the order of 10% (Strong et al., 1985).

## 3. Temporal analysis of PSR 0531 + 21

The arrival times of the selected gamma rays were transformed to Solar System Barycentric Time $T$ within an accuracy of 0.25 ms using the optical position of the pulsar (RA 82.88095; dec 21.9817778). The phase $\phi$ of each gamma ray was determined from the pulsar rotational frequency $f$ and its derivatives $\dot{f}, \ddot{f}$ at epoch $T_0$ according to

$$\phi = \phi_0 + \Delta T f + \frac{1}{2}\Delta T^2 \dot{f} + \frac{1}{6}\Delta T^3 \ddot{f}$$

where $\Delta T = T - T_0$ and $\phi_0$ is the phase offset. For observations 0, 14, 39 and 64 radio parameters were available for an epoch close to the observation period (Gullahorn et al., 1977, and private communications from V. Boriakoff and D. Ferguson, J.M. Rankin, and A.G. Lyne). For observation 54 the parameters were determined by scanning the data from a 2-12 keV X-ray detector on-board COS-B, while for observation 44 the actual gamma ray data was scanned about an extrapolation of the parameters from another epoch. The long duration of observation 64 (68 days) results in a degradation of the pulsar lightcurve when a single set of radio parameters are used for the analysis. Subsequently the data set for this observation were subdivided into 3 time intervals for which 3 corresponding sets of radio parameters were used. The pulsar parameters are given in Table 2.

**Table 2.** Timing parameters of PSR 0531 + 21 used for analysis of data

| Obs. period | Epoch JD-2440000 | $f$ ($s^{-1}$) | $\dot{f}$ ($10^{-10}\,s^{-2}$) | $\ddot{f}$ ($10^{-20}\,s^{-3}$) | Offset $\phi_0$ |
|---|---|---|---|---|---|
| 0 | 2647.0 | 30.13744554816328 | −3.8348446531 | 1.1413101714 | 0.352344 |
| 14 | 2982.0625 | 30.12634886 | −3.8310414 | 0.3956 | 0.376843 |
| 39 | 3946.442 | 30.094467179 | −3.82125043 | 1.225 | 0.958065 |
| 44 | 4128.5 | 30.088458052 | −3.81956 | 1.224 | 0.86 |
| 54 | 4508.5 | 30.075925066 | −3.81527838 | 1.22 | 0.85 |
| 64 | 5015.500000167454 | 30.05922409965165 | −3.81011540574 | 0.965891824 | 0.579803 |
| 64 | 5043.500000145255 | 30.05830242482511 | −3.80960798375 | 0.965664183 | 0.580751 |
| 64 | 5074.500000244583 | 30.05728207409174 | −3.80936211028 | 0.965572313 | 0.573312 |

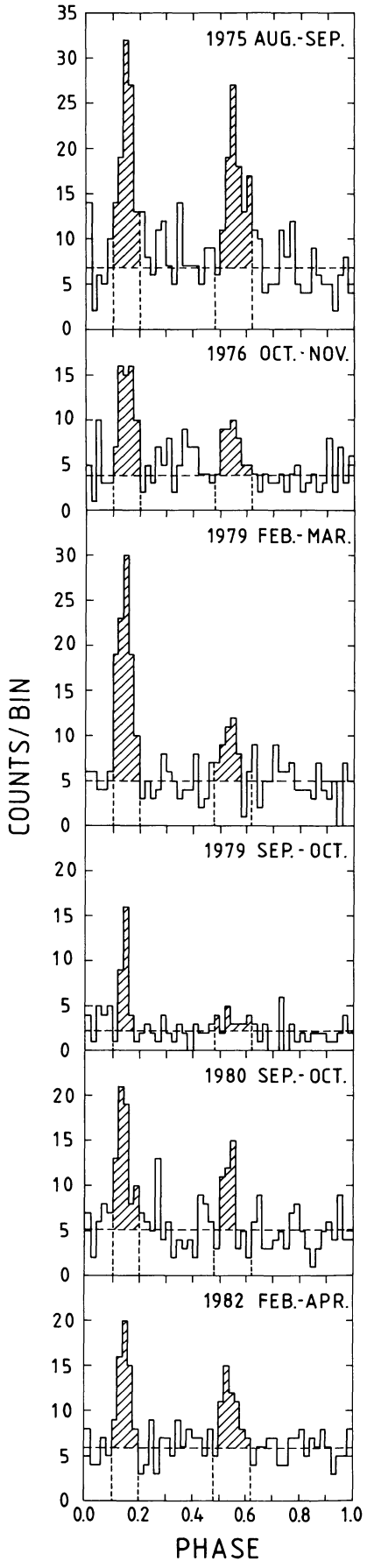


**Fig. 1.** The gamma ray phase histograms from PSR 0531 + 21 during each of the COS-B observations. Background levels and phase boundaries are indicated

In order to generate phase histograms, gamma rays were selected over an energy range of 50 MeV to 3000 MeV from within an energy dependent cone of half angle

$$\theta_{max} = 12.5\,E^{-0.16}(\text{degrees})$$

about the pulsar position. This expression optimises the gamma ray 'signal to noise ratio' for the energy dependent instrumental point-spread-function (Buccheri et al., 1983). Figure 1 shows the resultant phase histograms for each observational period. The variation in the background level represents not only the difference in useful observation time but also the angular dependence of the effective sensitive area and the gradual degradation of relative instrumental efficiency from 1.0 at observation 0 to 0.55 at observation 64. The summation of the individual phase histograms yields Fig. 2 which represents all COS-B observations of the Crab region. The separation and widths of the two peaks have been measured by Wills et al. (1982) and are found to be consistent with corresponding measurements at other wavelengths. In

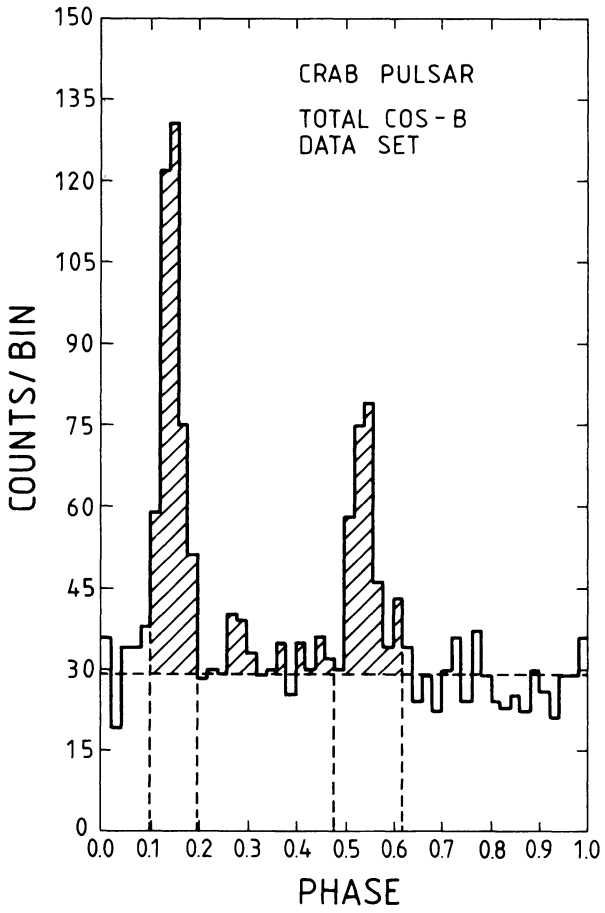


**Fig. 2.** The resultant phase histogram from the summation of the six observations given in figure 1

**Table 3.** Definition of phase intervals of Crab pulsar

| Region | Phase interval |
|---|---|
| First pulse | 0.10–0.20 |
| Inter-region | 0.20–0.48 |
| Second pulse | 0.48–0.62 |
| Background | 0.62–0.10 |

the region between the peaks evidence exists for 'interpulse' emission from the pulsar. This is consistent with observations at X-ray energies where a significant fraction of the total pulsed emission comes from this region (Pravdo and Serlemitsos, 1981). For detailed analysis of the pulsar emission the phase histogram has been divided into four regions as given in Table 3. These values are the same as those used by Wills et al. (1982) in analysis of COS-B data. The definition of these phase intervals is somewhat arbitrary and is chosen solely for the COS-B data analysis.

An examination of Fig. 1 indicates a possible relative temporal variation in the count rate of the two pulses. This effect has been reported previously by Wills et al. (1982) and Özel and Mayer-Hasselwander (1984). The number of gamma rays in each pulse (above the background) was determined using the 'saturation method' described by Bennett et al. (1977). The integral COS-B point-spread-function (Hermsen, 1980) for the appropriate energy range and Crab aspect angle was fitted to the total number of pulsed counts. Figure 3 shows the ratio of the strengths of the two pulses for each observation during the period from 1975 to 1982. Assuming that the data are Gaussian distributed a $\chi^2$ test has been made to determine if the deviations of the ratios are consistent with statistical fluctuations about a common mean. The results give a probability of 0.07 for statistical variability in the pulse ratios. However, this method only tests for the magnitude of the fluctuations and does not test for a trend in the ordering of the data points. This is achieved by using the run test (see for example Eadie et al., 1971). As these two tests are independent the overall distribution of the data is given by a combination of the two probabilities. This increases the probability that the variability of the pulse ratios is due to statistical fluctuations to 0.09. The results of the SAS-2 measurements of the Crab pulsar at energies above 35 MeV during 1972–1973 show the second pulse with slightly greater strength than the first. The pulse ratio for this observation has been determined by Wills et al. (1982) and is found to be $1.33 \pm 0.39$. Combining the SAS-2 result with those from COS-B gives a probability of 0.01 that the distribution of the data is due to statistical fluctuations. This result cannot be attributed to a change in the instrument response during the lifetime of the experiment, unless this change was energy dependent and a difference in the spectral index of the two pulses existed. In Sect. 4 it is shown that the differential spectrum of both pulses may be well represented by a single spectral index value. (It should be noted that for observation 64 the difference in the pulse ratio from that shown by Özel and Mayer-Hasselwander arises from the use of a single set of timing parameters to derive the phase histogram).

Using the instrument's calibration parameters, the effective sensitive area was determined for each observation over an energy range of 50 MeV to 3000 MeV for an assumed source spectral index of 2.00 (this is the value determined for the total pulsed emission). Figure 4 shows the resultant temporal behaviour of the flux from each pulse and the total pulsed emission during the period 1975–1982. The errors indicated in the figure are due only to statistics and do not include uncertainties in the value of the relative instrument sensitivity used for each observation. These uncertainties are less than 10% along the whole galactic plane (Strong et al., 1985). However, in the region of the Crab there are many overlapping observations and a more realistic estimate of the uncertainty for these observations is 5%. The first pulse shows fluctuation features with the flux reaching a maximum of $3.7\,10^{-6}$ photons/cm$^2$ s in February-April 1979 and a minimum of $1.7\,10^{-6}$ photons/cm$^2$ s in February-April 1982. For the second pulse, the decrease in strength noted by Wills et al. (1982) is clearly observed, and for the remaining observations the flux remains constant within the statistical uncertainties. The mean flux values above 50 MeV over all observations are $2.50 \pm 0.14\,10^{-6}$ photons/cm$^2$ s for the first pulse and $1.39 \pm 0.13\,10^{-6}$ photons/cm$^2$ s for the second pulse. The total pulsed emission also shows fluctuations features which are dominated by those from the first pulse. Assuming a value of 5% for the uncertainty in the relative instrument sensitivity the chance probability of these features being due to statistical fluctuations about a common mean value has been estimated to be 0.06 for the first pulse, 0.01 for the second pulse and 0.20 for the total pulsed emission. A linear correlation method has been used to search for correlation between the fluctuations observed from the different pulsar phase regions. The calculated value of $-0.35$ for the correlation coefficient indicates that there is no statistical evidence for such between the fluctua-

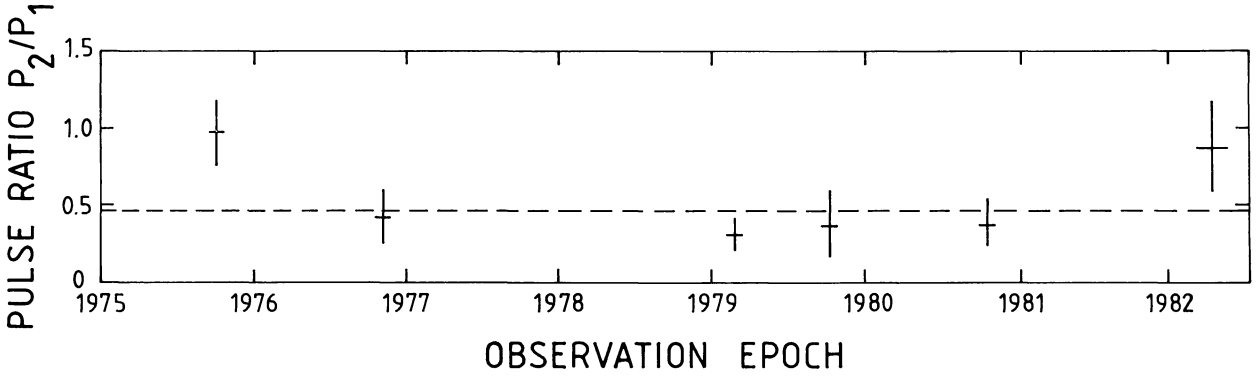


**Fig. 3.** Temporal variation of the counts ratio of second pulse to the first pulse over an interval from 1975 to 1982 in the energy range 50–3000 MeV

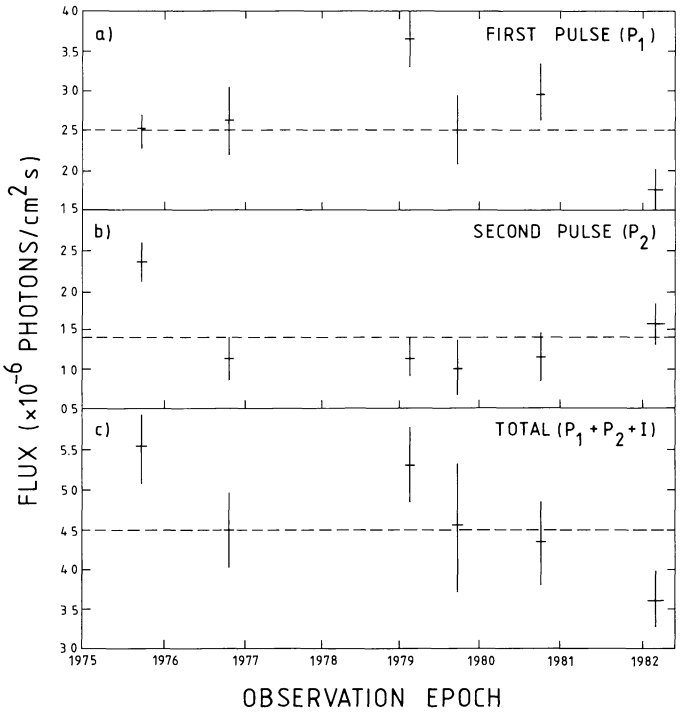


**Fig. 4a–c.** Temporal variation of the gamma ray flux above 50 MeV from **a** the first pulse **b** the second pulse and **c** the total pulsed emission. Only statistical errors are indicated

tions from either of the two pulses and the remainder of the pulsed emission. Table 4 shows the pulse ratios and flux values during each observation.

## 4. Energy spectrum of the pulsed emission from PSR 0831 + 21

In order to calculate the differential energy spectrum of PSR 0831 + 21 the data set was sub-divided into 6 energy intervals. In Fig. 5 the resultant phase histograms for each of the energy intervals is shown and pulsed gamma ray emission is seen up to an energy of 3 GeV. Using the same method as described in Sect. 3 the actual number of pulsed counts was determined for each energy interval. Using the energy dispersion probability and sensitive area of the instrument the count rate spectrum was deconvolved to give the actual differential energy spectrum of the pulsar. Figure 6 shows the derived pulsed spectrum for the combined emission from both pulses and the inter-region (see Table 3). The data can be well represented by a single power law of

$$F(E) = (2.86 \pm 0.50)\, 10^{-7} E^{-2.00 \pm 0.10} \text{ photons/cm}^2 \text{ s GeV}$$

The combined observations provide sufficient data to make a detailed measurement of the energy spectrum of the three emission regions defined in Table 3. The results are shown in Fig. 7. The individual spectra are seen to agree within the statistical uncertainties with the spectral index calculated for the total emission from the pulsar. The derived spectral indices from the individual data have values of $2.08 \pm 0.13$ for the first pulse $1.99 \pm 0.17$ for the second pulse and $1.98 \pm 0.32$ for the inter region.

## 5. The unpulsed gamma ray emission from the Crab region

Lichti et al. (1980) reported the detection of unpulsed emission from the Crab region up to an energy of 400 MeV using the data from the first two COS-B observations. This emission was found to contribute $45 \pm 10\%$ to the total emission. In order to determine the differential energy spectrum of the steady emission, skymaps of the pulsed and unpulsed emission from the Crab were generated for four energy intervals. The background region defined in Table 3 is used to represent the unpulsed emission, while the remainder of the pulsar cycle is taken as being pulsed. Figure 8 shows the resulting longitudinal profiles determined by summing the flux in galactic latitude over a region centered on the pulsar position. The extent of the latitude summation is determined by the instrument's point-spread-function over the particular energy range and is indicated in the figure. The angular width of the point-spread-function is seen to decrease with increasing energy. Using a method similar to that described by Kanbach et al. (1980) the total flux from the pulsed profile $F_p$ and the total flux from the unpulsed profile $F_{up}$ may be expressed as

$$F_p = P + f(S + B)$$
$$F_{up} = (1 - f)(S + B)$$

where $P$ is the flux from the pulsar, $S$ is the unpulsed source flux, $B$ is the diffuse galactic background and $f$ is the duty cycle of the pulsar. The combination of the pulsed and unpulsed longitudinal profiles gives the total gamma ray emission from the Crab region in each energy range. Assuming that the background flux may be well represented by the emission from the regions outside the point-spread-function then a test may be made using the pulsed and unpulsed profiles for the value $\alpha$ such that

$$\alpha = S/P$$

**Table 4.** Relative pulse strengths and flux values (50–3000 MeV) during each observation

| Observation period | 0 | 14 | 39 | 44 | 54 | 64 |
|---|---|---|---|---|---|---|
| Pulse ratio $P_2/P_1$ | $0.96 \pm 0.19$ | $0.43 \pm 0.17$ | $0.32 \pm 0.09$ | $0.39 \pm 0.21$ | $0.39 \pm 0.15$ | $0.91 \pm 0.29$ |
| Pulse flux ($10^{-6}$ photons/cm$^2$ s) | | | | | | |
| $P_1$ | $2.54 \pm 0.27$ | $2.63 \pm 0.41$ | $3.65 \pm 0.31$ | $2.51 \pm 0.44$ | $2.96 \pm 0.38$ | $1.73 \pm 0.28$ |
| $P_2$ | $2.35 \pm 0.24$ | $1.13 \pm 0.26$ | $1.15 \pm 0.23$ | $0.99 \pm 0.36$ | $1.14 \pm 0.29$ | $1.57 \pm 0.25$ |
| $P_1 + P_2 + I$ | $5.54 \pm 0.41$ | $4.47 \pm 0.46$ | $5.30 \pm 0.46$ | $4.52 \pm 0.79$ | $4.31 \pm 0.48$ | $3.59 \pm 0.34$ |

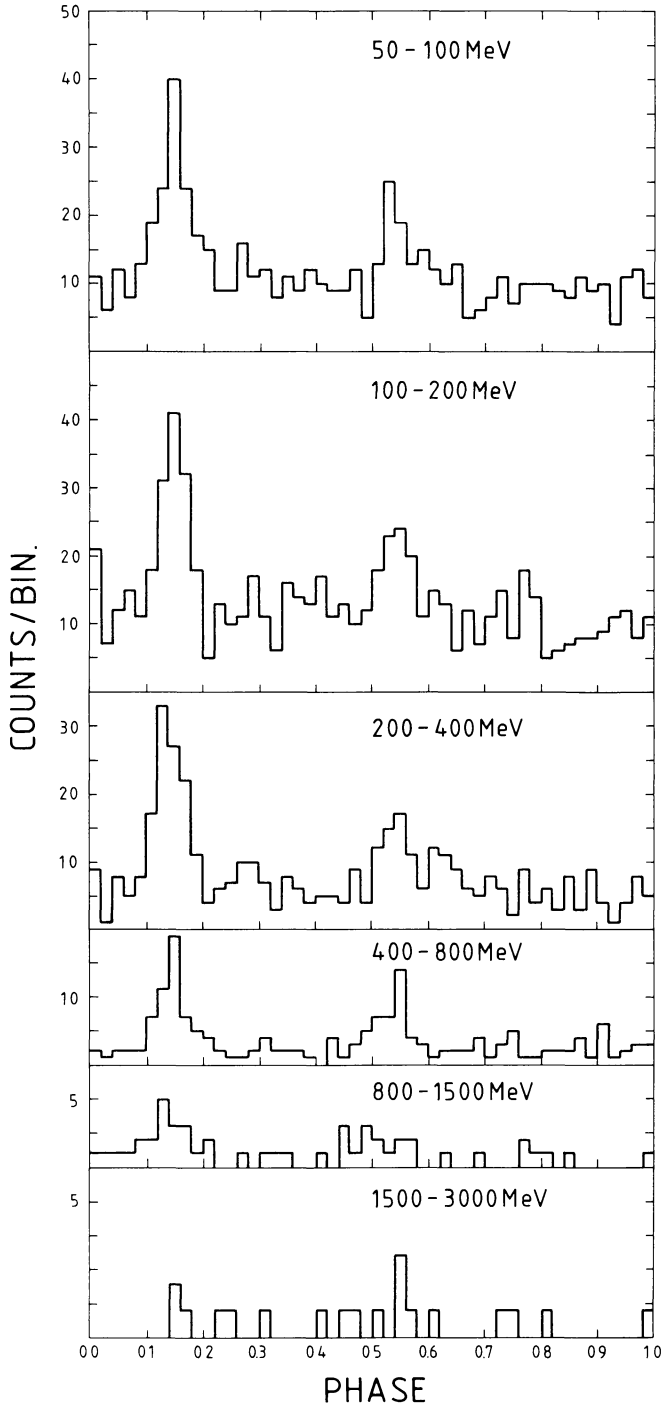


**Fig. 5.** Phase histograms of the total gamma ray emission over all observations in six energy intervals

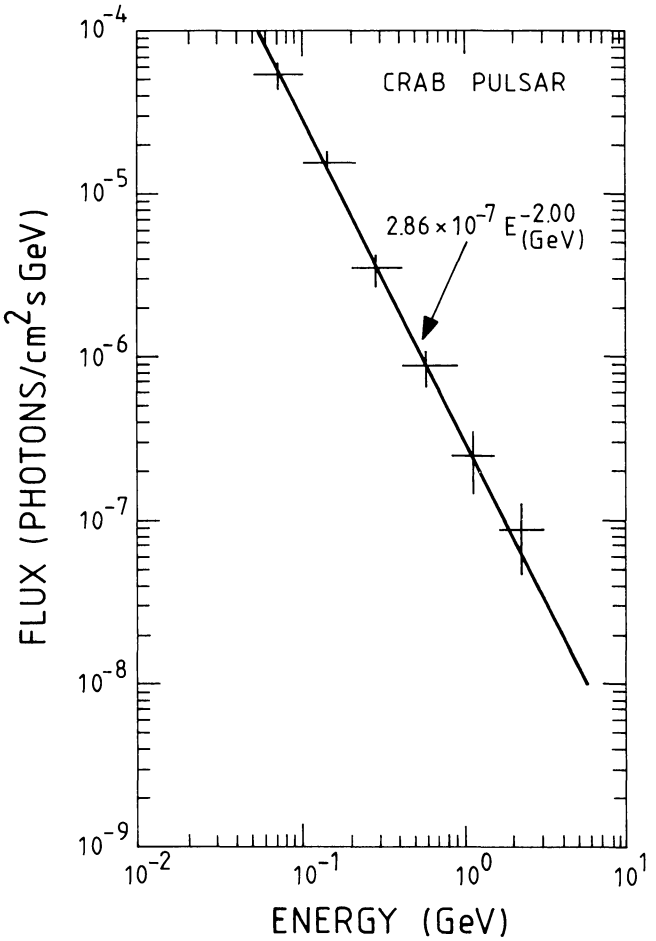


**Fig. 6.** The differential pulsed spectrum from PSR 0531 + 21. The line is a maximum likelihood fit to the data. Only statistical errors are indicated

The value $P$ has been determined for each energy interval by using the energy spectrum of the pulsar given in Sect. 4. Table 5 shows the derived values of $\alpha$ and the corresponding value of the steady gamma ray flux $S$ from the Crab region for each energy interval. Figure 9 shows the resultant differential energy spectrum. This has been fitted with a single power law spectrum of

$$F(E) = (0.63 \pm 0.25)\,10^{-7}\,E^{-2.7\pm0.3}\ \text{photons/cm}^2\,\text{s GeV}$$

It should be noted that this emission may not be entirely attributed to the Crab nebula as the angular resolution of COS-B is not sufficient to discriminate the entended nebula emission from a possible steady component from the pulsar. However, results from X-ray observations show the pulsar completely 'switched off" during the background phase interval (Harnden, 1983).

## 6. Discussion and conclusions

The extensive observations by COS-B of the galactic anti-centre region have facilitated a detailed study of the gamma ray emission from the Crab pulsar and nebula. With a total exposure of

**Table 5.** Calculated values of parameter $\alpha$ and d.c. flux values

| Energy interval (MeV) | $\alpha$ | Steady flux $S$ (photons/cm$^2$ s GeV) |
|---|---|---|
| 50–100 | $1.67 \pm 0.50$ | $9.55 \pm 5.67\,10^{-5}$ |
| 100–200 | $1.13 \pm 0.35$ | $1.62 \pm 0.92\,10^{-5}$ |
| 200–500 | $0.33 \pm 0.16$ | $9.44 \pm 6.89\,10^{-7}$ |
| 500–3000 | $< 0.60\ (2\sigma)$ | $< 1.15\,10^{-7}$ |

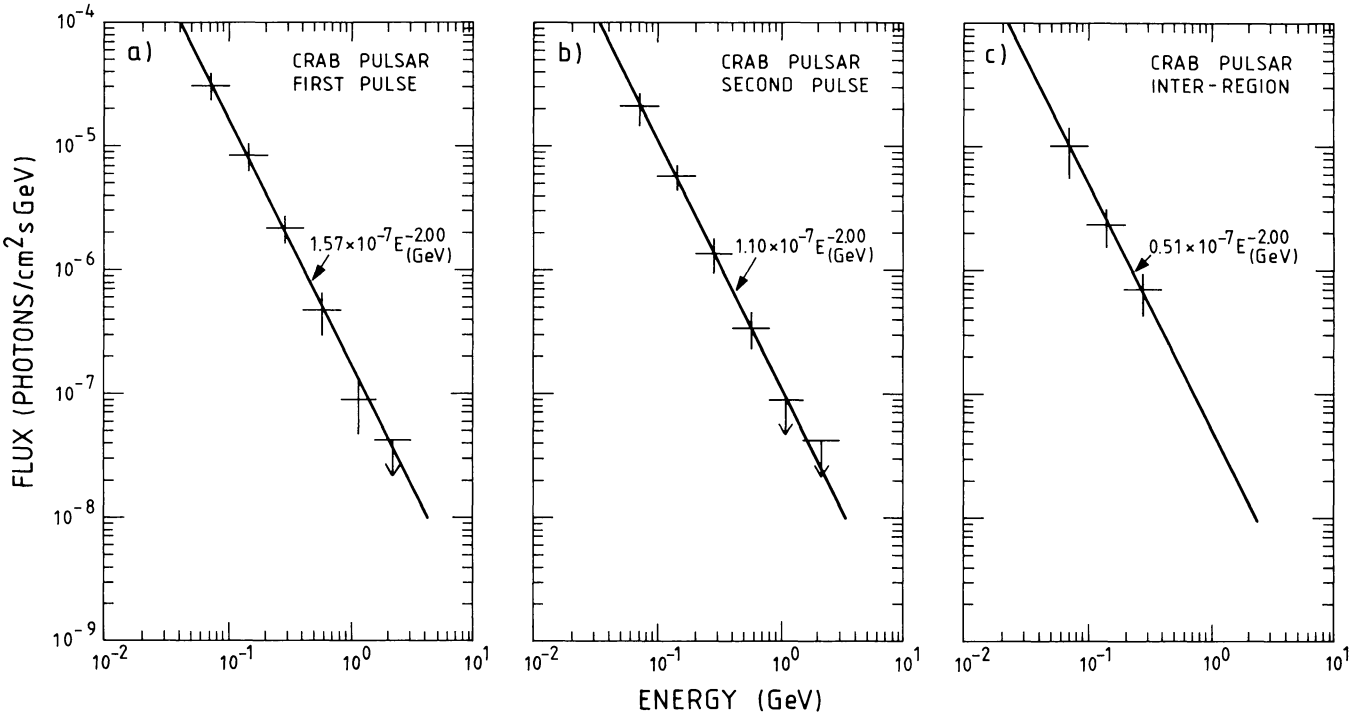


**Fig. 7a–c.** The differential spectrum from **a** the first pulse **b** the second pulse and **c** the interpulse. The lines are fits to the data for an assumed spectral index of 2.00

$1.5\,10^8$ cm$^2$ s this gives the largest gamma ray data-set on this object in the energy range 50 MeV–3000 MeV. This quantity and quality of data will not be equalled until the launch of NASA's Gamma Ray Observatory at the end of this decade. The emission from the Crab region consists of two components: a steady component which accounts for $53 \pm 15\%$ of the total emission and a pulsed component which accounts for $47 \pm 12\%$ over the energy range 50 MeV to 500 MeV. These values are consistent with previously reported estimates of Lichti et al. (1980) for COS-B observations from 50–400 MeV and Thompson et al. (1977) for SAS-2 observations from 35–200 MeV. The pulsar emission is dominated by two large peaks. The position of these peaks corresponds with radio, optical and X-ray measurements (Wills et al., 1982). In the inter-region between the peaks significant gamma ray emission exists. Averaged over all observations the relative strengths of each pulsed emission region are $50 \pm 9\%$ for the first pulse, $34 \pm 8\%$ for the second pulse and $16 \pm 5\%$ for the interpulse region.

The probability that the variability in the pulse ratio is due to statistical fluctuations has been estimated to be 0.09. This decreases to 0.01 when the additional observation from the SAS-2 experiment is included. The mean pulse ratio over all observations is $0.44 \pm 0.06$. It should be noted that at lower energies (0.5 MeV to 30 MeV) the phase histogram of Graser and Schönfelder (1982) shows both peaks with comparatively equal strength during balloon flights in October 1977 and May 1979, and data from the 2-12 keV X-ray 'pulsar synchronizer' on-board COS-B show no relative change in the lightcurve for observation periods 0, 39 and 54 (Wills et al., 1982).

Analysis of the flux from the different phase intervals indicates fluctuations as a function of time. However, the estimated uncertainty of 5% in the instrument sensitivity reduces the statistical significance of the features to $2.0\sigma$ for the first pulse, $3.0\sigma$ for the second pulse and $1.3\sigma$ for the total pulsed flux. No evidence for a correlation between the fluctuations from the different phase regions of the pulsar emission has been observed.

The pulsed spectrum from the Crab pulsar may be represented over the energy range 50 MeV–3000 MeV by a single power law with spectral index $2.00 \pm 0.10$. This result agrees within the statistical errors with previous COS-B results of Bennett et al. (1977) and Lichti et al. (1980). The differential energy spectrum from the three pulsed emission regions (see Table 2) are each well fitted with the spectral index value calculated for the total pulsed emission and there is no indication in the data of a systematic variation in spectral index with the pulsar phase as has been reported at hard X-ray energies by Pravdo and Serlemitsos (1981) and by Knight (1982). The results indicate that for the interpulse emission a significant increase in the value of the spectral index must occur in the hard X-ray to medium gamma ray energy range. With a spectral index of 1.63 (Knight, 1982) the extrapolated interpulse flux lies at least one order of magnitude above the value observed by COS-B. An extrapolation of the total spectrum to hard X-ray and medium energy gamma ray energies gives good agreement to within the statistical uncertainties with other observations (Pravdo and Serlemitsos, 1981; White et al., 1985; Graser and Schönfelder, 1982). However, at very high energies (1 TeV) the extrapolated spectrum is one order of magnitude greater than the flux reported from ground-based atmospheric Čerenkov experiments (Porter and Weekes, 1978). There is no indication in the pulsed spectrum of any change in the spectral index up to an energy of 3 GeV.

The steady gamma ray emission spectrum from the Crab region has been determined and is found to be consistent up to 500 MeV with a power law spectrum of index $2.7 \pm 0.3$. Recent

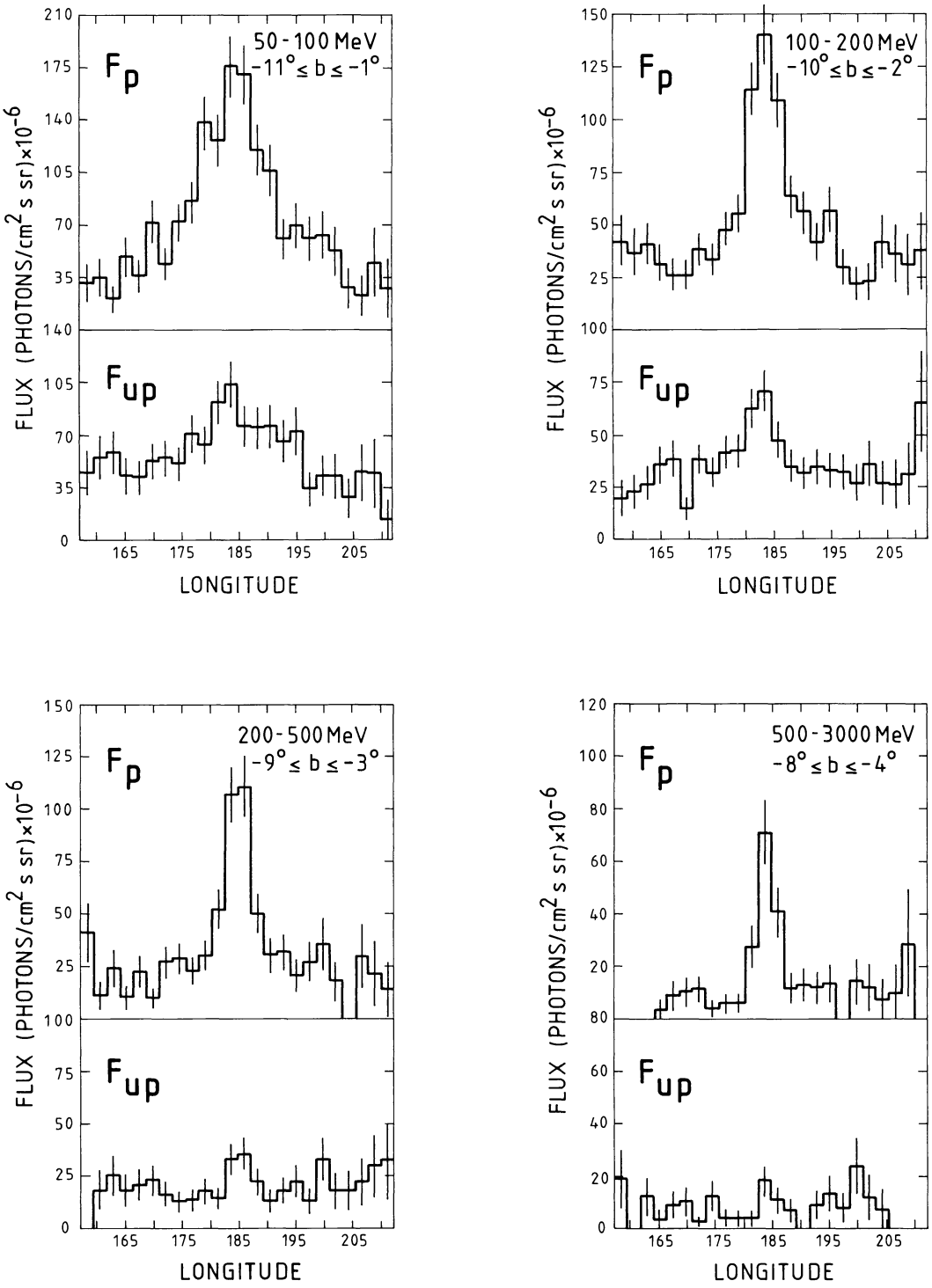


**Fig. 8.** Galactic longitudinal profiles of the pulsar and nebular gamma ray emission for four energy intervals: 50–100 MeV; 100–200 MeV; 200–500 MeV; 500–3000 MeV. The extent of the galactic latitude summation is indicated and is chosen to maximize the signal-to-noise of the profiles

results from HEAO A-4 observations (Jung, 1986) indicate a break in the spectrum from the nebular emission at an energy of 150 keV with the spectral index increasing from $2.13 \pm 0.05$ to $2.54 \pm 0.08$ and is in agreement within the statistical uncertainties with the value calculated from the present data. The extrapolated spectrum of Jung is indicated in Fig. 9. Both data sets are in good agreement, thus supporting the spectral break at hard X-ray energies and the continuation of the softer spectrum up to 500 MeV. However, due to the poor spatial resolution of both HEAO A-4 and COS-B experiments this spectrum may contain a contribution from a possible steady emission from the pulsar during the non-pulsed phase interval. At very high energies,

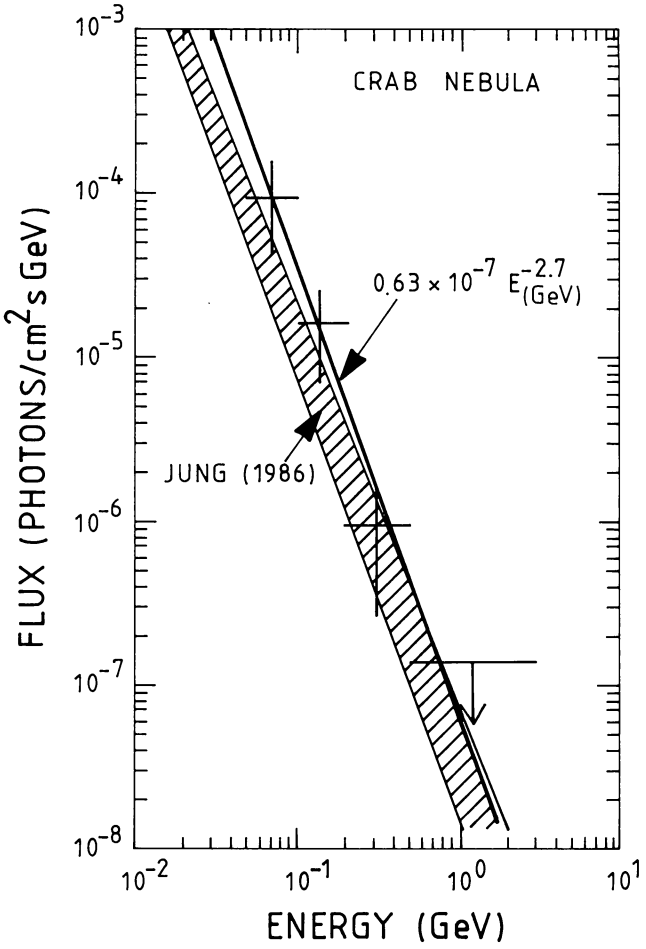


**Fig. 9.** The differential spectrum of the Crab nebula. The solid line is the maximum likelihood fit to the data. The shaded area is an extrapolation of the energy spectrum from hard X-ray energies (Jung, 1986)

above 500 GeV, there have been reports of the detection of non-pulsed gamma ray emission from the Crab region at flux levels of $\sim 5\,10^{-11}$ photons/cm$^2$s (Fazio et al., 1972; Cawley et al., 1985). An extrapolation of the spectrum derived above gives a value which is more than an order of magnitude below the reported flux value.

*Acknowledgements.* We wish to thank Drs J.M. Rankin, V. Boriakoff, D. Ferguson and A.G. Lyne for the communication of unpublished radio data. J. Clear acknowledges receipt of a research fellowship from the European Space Agency. The Laboratory for Space Research Leiden is supported financially by ZWO, the Netherlands Organisation for the Advancement of Pure Research.

## References

Albats, P., Frye, G.M., Jr., Mace, O.B., Hopper, V.D., Thomas, J.A.: 1972, *Nature* **240**, 221

Bennett, K., Bignami, G.F., Boella, R., Buccheri, R., Hermsen, W., Kanbach, G., Lichti, G.G., Masnou, J.L., Mayer-Hasselwander, H.A., Paul, J.A., Scarsi, L., Swanenberg, B.N., Taylor, B.G., Wills, R.D.: 1977, *Astron. Astrophys.* **61**, 279

Browning, R., Ramsden, D., Wright, P.J.: 1971 *Nature* **232**, 99

Buccheri, R., Bennett, K., Bignami, G.F., Bloemen, J.B.G.M., Boriakov, V., Caraveo, P.A., Hermsen, W., Kanbach, G., Manchester, R.N., Masnou, J.L., Mayer-Hasselwander, H.A., Ozel, M.E., Paul, J.A., Sacco, B., Scarsi, L., Strong, A.W.: 1983, *Astron. Astrophys.* **128**, 245

Cawley, M.F., Fegan, D.J., Gibbs, K., Gorham, P.W., Lamb, R.C., Liebing, D.F., MacKeown, P.K., Porter, N.A., Stenger, V.J., Weekes, T.C.: 1985, Proc. 19th Int. Cosmic Ray Conf., La Jolla, USA, **1**, 131

Dowthwaite, J.C., Harrison, A.B., Kirkman, I.W., Macrea, H.J., McComb, T.J.L., Orford, K.J., Turver, K.E., Walmsley, W.: 1985, *Astrophys. J.*, **286**, L35

Eadie, W.T., Drijard, D., James, F.E., Roos, M., Sadoulet, B.: 1971, Statistical Methods in Experimental Physics, North Holland, p. 230–232

Fazio, G.G., et al.: 1972, *Astrophys. J. Letters*, **175**, L117

Gullahorn, G.T., Isaacman, R., Rankin, J.M., Payne, J.J.: 1977, *Astron. J.* **82**, 309

Graser, U., Schönfelder, V.: 1982, *Astrophys. J.*, **263**, 677

Greisen, K., Ball, S.E., Cambell, M., Gilman, D., Strickman, M., McBreen, B., Koch, D.: 1975, *Astrophys. J.*, **197**, 471

Harnen, F.R.: 1983, Supernova Remnants and their X-Ray Emission, p. 131. (eds. Danziger, J. and Gorenstein, P., IAU)

Hasinger, G.: 1984, Proc Int. Symp. on X-ray Astron., Bologna, p. 305

Haymes, R.C., Glenn, S.W., Fishman, G.J., Harnden, F.R.: 1969, *J. Geophys. Res.*, **74**, 5792

Hermsen, W.: 1980, Ph.D. thesis, Univ. Leiden

Jung, G.V.: 1986, Ph.D. thesis, Univ. of California, San Diego

Kanbach, G., Bennett, K., Bignami, G.F., Buccheri, R., Caraveo, P., D'Amico, N., Hermsen, W., Lichti, G.G., Masnou, J.L., Mayer-Hasselwander, H.A., Paul, J.A., Sacco, B., Swanenberg, B.N., Wills, R.D.: 1980, *Astron. Astrophys.* **90**, 163

Kniffen, D.A., Hartman, R.C., Thompson, D.J., Bignami, G.F., Fichtel, C.E., Ogelman, H., Tumer, T.: 1974, *Nature* **251**, 397

Knight, F.K.: 1982, *Astrophys. J.* **260**, 538

Knudt, W., Krotscheck, E.: 1980, *Astron. Astrophys.* **83**, 1

Laros, J.G., Matteson, J.L., Pelling, R.M.: 1973, *Nature Phys. Sci.* **246**, 109

Lichti, G.G., Buccheri, R., Caraveo, P., Gerardi, G., Hermsen, W., Kanbach, G., Masnou, J.L., Mayer-Hasselwander, H.A., Paul, J.A., Swanenburg, B.N., Wills, R.D.: 1980, Non-Solar Gamma Rays, Advances in Space Exploration Vol. 7 p. 49 (eds. Cowsik, R. and Wills, R.D. Pergamon, Oxford)

Mayer-Hasselwander, H.A.: 1985, Explanatory Supplement to the COS-B Final Database

Mayer-Hasselwander, H.A., Bennett, K., Bignami, G.F., Bloemen, J.G.B.M., Buccheri, R., Caraveo, P.A., Hermsen, H., Kanbach, G., Lebrun, F., Paul, J.A., Sacco, B., Strong, A.W.: 1985, Proc. 19th Int. Cosmic Ray Conf., La Jolla, USA, **3**, 383

McBreen, B., Ball, S.E., Cambell, M., Greisen, K., Koch, D.: 1973, *Astrophys. J.* **184**, 571

Özel, M.E., Mayer-Hasselwander, H.A.: 1984, Inter. Workshop on Data Analysis in Astronomy, Erice, Italy

Porter, N.A., Delaney, T., Weekes, T.C.: 1974, Proc 9th ESLAB Symp., ESRO SP-106, 295

Porter, N.A., Weekes, T.C.: 1978, Smithsonian Ap. Obs. Spec. Rept., No. 381

Pravdo, S.H., Serlemitsos, P.J.: *Astrophys. J.* **246**, 484
Strong, A.W., Bloemen, J.B.G.M., Buccheri, R., Hermsen, W., Lebrun, F., Mayer-Hasselwander, H.A.: 1985, Proc. 19th Int. Cosmic Ray Conf., La Jolla, USA, **3**, 387
Thompson, D.J., Fichtel, C.E., Hartman, R.C., Kniffen, D.A., Lamb, R.C.: 1977, *Astrophys. J.* **213**, 252
Toor, A., Seward, F.D.: 1974, *Astron. J.* **79**, 995
Trimble, V.: 1968, *Astron. J.* **73**, 535
Walraven, G.D., Hall, R.D., Meegan, C.A., Coleman, P.L., Shelton, D.H., Haymes, R.C.: 1975, *Astrophys. J.* **202**, 502
White, R.S., Sweeney, W., Tumer, T., Zych, A.: 1985, *Astrophys. J.* **299**, L23
Wills, R.D., Bennett, K., Bignami, G.F., Buccheri, R., Caraveo, P.A., Hermsen, W., Kanbach, G., Masnou, J.L., Mayer-Hasselwander, H.A., Paul, J.A., Sacco, B.: 1982, *Nature* **296**, 723